PROCEEDINGS OF SCIENCE

Global flavour fits to rare B decay observables

F. Mahmoudi,[a,*] **T. Hurth**[b] **and S. Neshatpour**[a]

[a] *Université de Lyon, Université Claude Bernard Lyon 1, CNRS/IN2P3, Institut de Physique des 2 Infinis de Lyon, UMR 5822, F-69622, Villeurbanne, France*

[b] *PRISMA+ Cluster of Excellence and Institute for Physics (THEP), Johannes Gutenberg University, D-55099 Mainz, Germany*

E-mail: mahmoudi@in2p3.fr

We explore the current status of decays involving $b \to s\ell^+\ell^-$ transitions. The recent LHCb update on measurements of R_K and R_{K^*} indicates compatibility with the Standard Model, restricting potential contributions from new physics to adhere to lepton flavour universality. In addition to the latest LHCb measurements of R_K and R_{K^*}, we incorporate recent CMS measurements of both R_K and the branching ratio of $B^+ \to K^+\mu^+\mu^-$. Our analysis adopts a model-independent approach to scrutinise the $b \to s\ell^+\ell^-$ data, examining the implications of various sets of observables. Furthermore, we explore multi-dimensional fits, assessing the significance of more complex new physics scenarios in comparison to simpler one- and two-dimensional scenarios.

20th International Conference on B-Physics at Frontier Machines (Beauty2023)
3-7 July, 2023
Clermont-Ferrand, France

*Speaker

PoS(BEAUTY2023)045

1. Introduction

Over the past decade, the LHCb collaboration has measured several decay modes with $b \to s\ell^+\ell^-$ transitions, and in particular, reported indications of lepton flavour non-universality at the 3σ level through measurements of the ratios R_K and R_{K^*} [1]. These ratios, defined as the branching fractions of $B \to K^{(*)}\ell^+\ell^-$ for muons compared to electrons, are theoretically robust with uncertainties below one percent and central values near unity in the Standard Model (SM) due to lepton flavour universality [2, 3].

Simultaneously, persistent tensions exist in the angular observables and branching ratios of exclusive $b \to s$ processes [4–12]. These exclusive decay observables depend on local matrix elements (form factors) and non-local contributions, posing challenges in distinguishing new physics (NP) effects from hadronic effects. While certain angular observables are less form factor-sensitive, they rely on non-local hadronic contributions, introducing uncertainties. Recent advancements in evaluating non-local contributions [13–16] suggest small non-factorisable power corrections.

Previously, the noteworthy aspect was the consistent description of deviations in clean ratios and angular observables with the same new physics scenarios. This consistency was reinforced by the updated measurement of $\mathrm{BR}(B_s \to \mu^+\mu^-)$ [17]. Combining this result with ATLAS and LHCb measurements [18–20], $\mathrm{BR}(B_s \to \mu^+\mu^-)\mathrm{exp}^{\mathrm{comb.}} = \left(3.52^{+0.32}{-}0.30\right) \times 10^{-9}$, as reported in [21], aligns with the SM within 1σ, mitigating substantial new physics contributions in the Wilson coefficient C_{10}. However, recent measurements by the LHCb collaboration reveal that the ratios are now in agreement with the Standard Model [22].

Here, we analyse the current situation in a model-independent way. The tensions in the angular observables and branching ratios have not changed by the new LHCb measurements. We analyse the two sets of $b \to s$ data separately, namely the theoretically clean ratios together with $\mathrm{BR}(B_{s,d} \to \ell^+\ell^-)$ on one side and the angular observables and branching ratios on the other side.

The complete list of the observables used in the present fits can be found in Refs. [21, 23]. We used the `SuperIso` public program [24, 25] assuming 10% uncertainty for the unknown non-factorisable power corrections (see Refs. [26, 27] for more details).

1.1 Fits to clean $b \to s\ell\ell$ observables

We first do the fits for the clean observables, namely $R_{K^{(*)}}$ and $\mathrm{BR}(B_{s,d} \to \mu^+\mu^-)$. In Table 1, we present the results of one-operator fits for these clean observables, both before (pre-$R_{K^{(*)}}$, as detailed in [21]) and after the most recent $R_{K^{(*)}}$ measurements (see Ref. [27]). As can be seen, the change is substantial, and only minor deviations from lepton universality are now permissible. Nevertheless, there remain lepton flavour universality violating (LFUV) ratios, $R_{K^0_S}^{\mathrm{LHCb}}([1.1-6.0])$, $R_{K^{*+}}^{\mathrm{LHCb}}([0.045-6.0])$ [28], and $R_K^{\mathrm{LHCb}}([1.1-6.0])$[22] with NP significance of 1.7, 1.4 and 1.1σ, respectively.

The results of two-operator fits are presented in Figure 1 which clearly show that the new data confirms lepton universality. The favoured regions in the case of $\{C_{10}^e, C_{10}^\mu\}$ are bounded along the diagonal because we have included $\mathrm{BR}(B_{s,d} \to \mu^+\mu^-)$ in the fit which implies strong constraints on C_{10} in general. In the plane $\{C_9^\mu, C_{10}^\mu\}$, the 1 and 2σ regions are now also grouped around the secondary diagonal and contain the SM values. Only small NP contributions are still possible after the new measurements. We note however that without $\mathrm{BR}(B_{s,d} \to \mu^+\mu^-)$ in the fit, i.e. without the

Only LFUV ratios and $B_{s,d} \to \ell^+\ell^-$ **pre-$R_{K^{(*)}}$ update** ($\chi^2_{\rm SM} = 30.63$)			
	b.f. value	$\chi^2_{\rm min}$	Pull$_{\rm SM}$
δC_9^e	0.83 ± 0.21	10.8	4.4σ
δC_9^μ	-0.80 ± 0.21	11.8	4.3σ
δC_{10}^e	-0.81 ± 0.19	8.7	4.7σ
δC_{10}^μ	0.50 ± 0.14	16.2	3.8σ
$\delta C_{\rm LL}^e$	0.43 ± 0.11	9.7	4.6σ
$\delta C_{\rm LL}^\mu$	-0.33 ± 0.08	12.4	4.3σ

Only LFUV ratios and $B_{s,d} \to \ell^+\ell^-$ **post-$R_{K^{(*)}}$ update** ($\chi^2_{\rm SM} = 9.37$)			
	b.f. value	$\chi^2_{\rm min}$	Pull$_{\rm SM}$
δC_9^e	0.17 ± 0.16	8.2	1.1σ
δC_9^μ	-0.18 ± 0.16	8.1	1.1σ
δC_{10}^e	-0.15 ± 0.14	8.3	1.1σ
δC_{10}^μ	0.15 ± 0.12	7.7	1.3σ
$\delta C_{\rm LL}^e$	0.08 ± 0.08	8.2	1.1σ
$\delta C_{\rm LL}^\mu$	-0.09 ± 0.07	7.7	1.3σ

Table 1: One operator NP fit to clean observables before and after update of $R_{K^{(*)}}$ measurement.

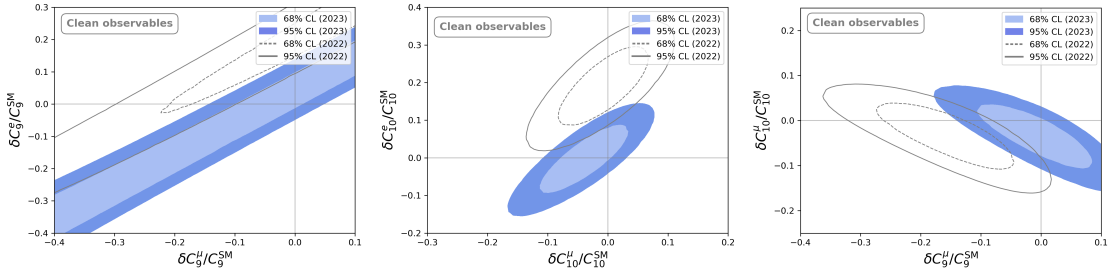

Figure 1: Two-dimensional fits to clean observables. The coloured regions correspond to the post-$R_{K^{(*)}}$ fits and the gray contours correspond to the fits prior to the recent $R_{K^{(*)}}$ update.

strong constrain on C_{10}^μ much larger values of C_9^μ and C_{10}^μ would be possible along the secondary diagonal. Such larger contributions are then in principle possible but due to unnatural cancellations of these two contributions in the ratios R_K and R_{K^*} only.

2. Fits to all $b \to s\ell\ell$ data except clean observables

In Table 2, we present the one-parameter fits for the remaining $b \to s$ observables, excluding the previously discussed clean observables. These fits exhibit almost no change compared to the situation prior to the new measurements of R_K and R_{K^*}. The slight variations in NP significance can be attributed to the recent measurements by CMS and updates of the CKM parameters [29].

However, when comparing the one-operator fits for the clean observables in Table 1 with those for the remaining $b \to s$ observables in Table 2, it becomes evident that there is no longer consistency for the non-universal Wilson coefficients C_9^μ and C_{LL}^μ. This implies that the substantial tensions persisting in the rest of the $b \to s$ observables, particularly in the angular observables and branching ratios, should be addressed using lepton-universal operators.

Three dimensional fits to angular observables and branching ratios (with the assumption of 10% power corrections) are shown in Figure 2.

All observables except LFUV ratios and $B_{s,d} \to \ell^+\ell^-$ **pre-$R_{K^{(*)}}$ update** ($\chi^2_{\rm SM} = 221.8$)			
	b.f. value	$\chi^2_{\rm min}$	Pull$_{\rm SM}$
δC_9	-0.95 ± 0.13	185.1	6.1σ
δC_9^e	0.70 ± 0.60	220.5	1.1σ
δC_9^μ	-0.96 ± 0.13	182.8	6.2σ
δC_{10}	0.29 ± 0.21	219.8	1.4σ
δC_{10}^e	-0.60 ± 0.50	220.6	1.1σ
δC_{10}^μ	0.35 ± 0.20	218.7	1.8σ
$\delta C_{\rm LL}^e$	0.34 ± 0.29	220.6	1.1σ
$\delta C_{\rm LL}^\mu$	-0.64 ± 0.13	195.0	5.2σ

All observables except LFUV ratios and $B_{s,d} \to \ell\bar{\ell}$ **post-$R_{K^{(*)}}$ update** ($\chi^2_{\rm SM} = 261.6$)			
	b.f. value	$\chi^2_{\rm min}$	Pull$_{\rm SM}$
δC_9	-0.97 ± 0.13	221.9	6.3σ
δC_9^e	0.70 ± 0.60	260.4	1.1σ
δC_9^μ	-0.98 ± 0.13	219.7	6.5σ
δC_{10}	0.36 ± 0.20	258.3	1.8σ
δC_{10}^e	-0.50 ± 0.50	260.5	1.0σ
δC_{10}^μ	0.41 ± 0.20	257.0	2.1σ
$\delta C_{\rm LL}^e$	0.31 ± 0.28	260.4	1.1σ
$\delta C_{\rm LL}^\mu$	-0.65 ± 0.12	231.7	5.5σ

Table 2: One operator fits for all except clean observables before (left) and also after (right) the LHCb-update of $R_{K^{(*)}}$.

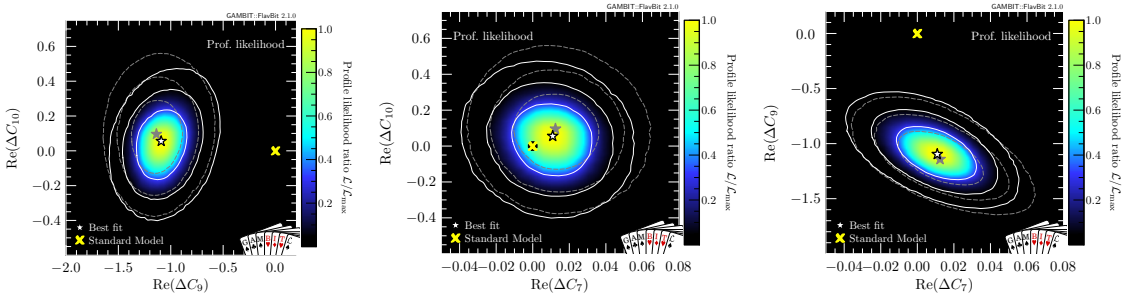

Figure 2: Combined fit to the C_7, C_9 and C_{10} Wilson coefficients. Contour lines indicate 1, 2 and 3σ confidence regions. White contours and coloured shading show the results where we compute theory covariances self-consistently for every combination of Wilson coefficients. Grey contours and curves show the corresponding result when we approximate the theory covariance by its value in the Standard Model, across the entire parameter space. The Standard Model prediction is indicated by a yellow cross. [30].

2.1 Fits to all $b \to s\ell\ell$ observables

We now consider the fits using all $b \to s$ observables, where we only take lepton-universal operators. The outcomes are detailed in Table 3, revealing that the favored universal coefficient is C_9 to reconcile the discrepancies observed in the angular observables and branching ratios. While, C_9^μ and C_{LL}^μ could account for these tensions, such contributions from new physics would not align with the constraints imposed by the clean observables, as demonstrated earlier.

Table 4 gives the one-operator fit results using chiral universal coefficients[1], revealing a substantial NP significance for fits involving C_{LL} and C_{LR}, that is, for left-handed quark currents.

In addition, we present the two-dimensional fit results in Figure 3. The right plot in the $\{C_9, C_{10}\}$ plane shows that not the universal coefficient C_{10} but C_9 explains the present anomalies best. This is also a consequence of the C_{10} dependence on the $B_s \to \mu^+\mu^-$ branching ratio which is SM-like. The plot on the left shows the two-operator fit to $\{C_9^\mu, C_{10}^\mu\}$. Compared to the pre-$R_{K^{(*)}}$ update, the 1 or 2σ ranges now move in the direction of the second diagonal to allow a partial

[1]Here $C_{LL} \equiv C_9 = -C_{10}$, $C_{RL} \equiv C_9' = -C_{10}'$ $C_{RR} \equiv C_9' = C_{10}'$ and $C_{LR} \equiv C_9 = C_{10}$.

All observables **pre-$R_{K^{(*)}}$ update** ($\chi^2_{\rm SM} = 253.5$)				All observables **post-$R_{K^{(*)}}$ update** ($\chi^2_{\rm SM} = 271.0$)			
	b.f. value	$\chi^2_{\rm min}$	Pull$_{\rm SM}$		b.f. value	$\chi^2_{\rm min}$	Pull$_{\rm SM}$
δC_7	-0.02 ± 0.01	248.7	2.2σ	δC_7	-0.02 ± 0.01	267.2	1.9σ
δC_{Q_1}	-0.05 ± 0.02	252.3	1.1σ	δC_{Q_1}	-0.04 ± 0.03	270.3	0.8σ
δC_{Q_2}	-0.01 ± 0.01	252.4	1.0σ	δC_{Q_2}	-0.01 ± 0.01	270.4	0.8σ
δC_9	-0.95 ± 0.13	215.8	6.1σ	δC_9	-0.96 ± 0.13	230.7	6.3σ
δC_{10}	0.08 ± 0.16	253.2	0.5σ	δC_{10}	0.15 ± 0.15	270.0	1.0σ

Table 3: One operator NP fits to all $b \to s\ell\ell$ observables before and after the update of $R_{K^{(*)}}$ by the LHCb collaboration.

All observables **post-$R_{K^{(*)}}$ update** ($\chi^2_{\rm SM} = 271.0$)			
	b.f. value	$\chi^2_{\rm min}$	Pull$_{\rm SM}$
$\delta C_{\rm LL}$	-0.54 ± 0.12	249.1	4.7σ
$\delta C_{\rm LR}$	-0.42 ± 0.10	257.4	3.7σ
$\delta C_{\rm RL}$	0.00 ± 0.08	268.8	1.5σ
$\delta C_{\rm RR}$	0.21 ± 0.13	268.1	1.7σ

Table 4: One operator fits to all $b \to s\ell\ell$ observables in the chiral basis.

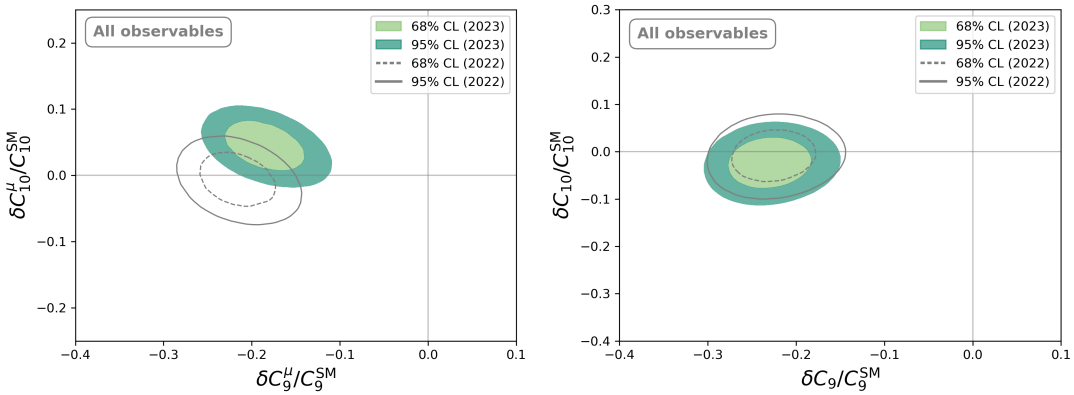

Figure 3: Two-dimensional fits to all observables.

compensation of the C_9^{μ} and the C_{10}^{μ} contributions within the $R_{K^{(*)}}$ ratios. Because of this unnatural compensation, this specific two-operator fit is important.

Next, we will have a closer look at the two-operator fits to $\{C_9^{\mu}, C_{10}^{\mu}\}$ and $\{C_9, C_{10}\}$. We consider the constraints imposed by the $R_{K^{(*)}}$ ratios separately from those arising from BR($B_{s,d} \to \mu^+\mu^-$). Additionally, for the remaining $b \to s\ell^+\ell^-$ observables, we evaluate the influence of low-q^2 and

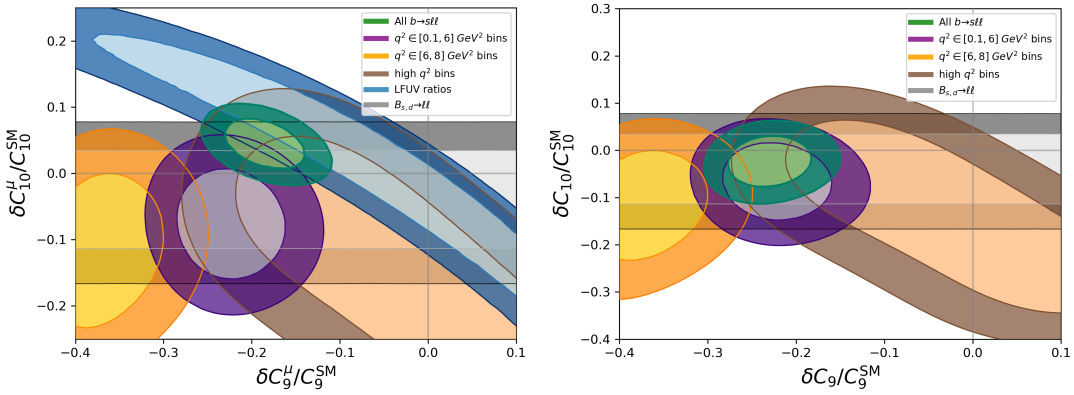

Figure 4: Two-dimensional fits to all observables in green. Where relevant, the impact of the $b \to s\ell\ell$ observables for the low q^2 bins up to 6 GeV^2, for the $[6,8]$ GeV^2 bin and for the high q^2 bins as well as the bounds from the lepton flavour universality violating ratios and $B_{s,d} \to \ell^+\ell^-$ are shown separately with the lighter (darker) shade indicating the 68% (95%) confidence level region.

high-q^2 bins separately.

Due to concerns about the validity of SCET in the low-q^2 bin $[6,8]$ GeV^2 (near the J/ψ resonance), we treat this bin distinctly from other low-q^2 bins up to 6 GeV^2. In Figure 4, we deconstruct the two-operator fits to illustrate the impact of each set of observables on the overall fit. In the right-hand plot, the $\{C_9, C_{10}\}$ two-operator fit is displayed, with brown contours representing the 1 and 2σ regions of the high-q^2 bins. These observables are compatible with SM values, albeit with relatively large uncertainties. The primary source of tensions in angular observables and branching ratios lies in the low-q^2 bins, as indicated by the purple contours. High-q^2 observables exhibit weak dependence on Wilson coefficients, resulting in low sensitivity to NP. The yellow contours demonstrate a substantial increase in NP significance when incorporating the highest low-q^2 bin from 6 to 8 GeV^2 into the fit. However, this pronounced effect may suggest the potential breakdown of SCET in this range. Finally, the grey contours arising from $B_{s,d} \to \mu^+\mu^-$ branching ratios constrain the Wilson coefficient C_{10}. In the left plot, we look at the bounds on $\{C_9^{\mu}, C_{10}^{\mu}\}$. The blue 1 and 2σ regions show the bounds generated by the ratios $R_{K^{(*)}}$. Much larger values of C_9^{μ} and also of C_{10}^{μ} are now allowed, however, this is possible due to an unnatural compensation between the C_9^{μ} and the C_{10}^{μ} contributions in the ratios which makes the $\{C_9^{\mu}, C_{10}^{\mu}\}$ fit problematic, as already mentioned above.

3. Comparison of global fit results

Here we present a comparison between global fits performed by the different fitting groups, where the results of the following groups have been confronted:

- ABCDMN: M. Algueró, A. Biswas, B. Capdevila, S. Descotes-Genon, J. Matias, M. Novoa-Brunet [31].

- AS: W. Altmannshofer, P. Stangl [32].

- CFFPSV: M. Ciuchini, M. Fedele, E. Franco, A. Paul, L. Silvestrini, M. Valli [33].

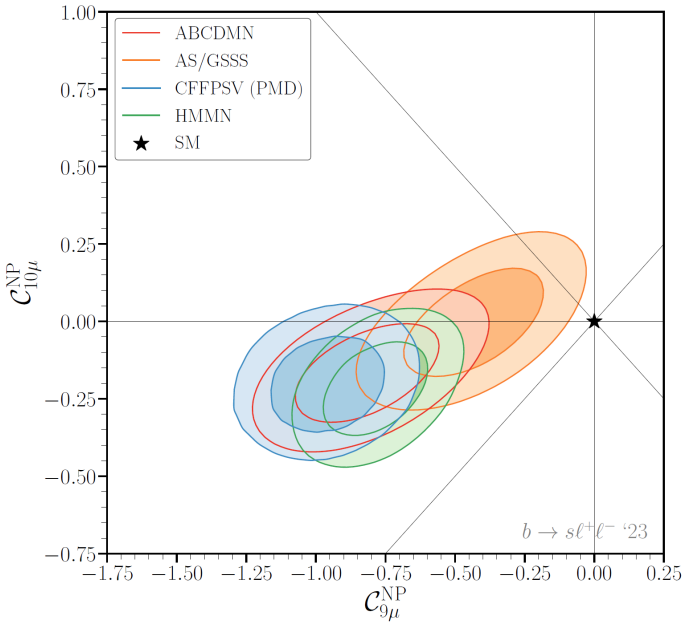

Figure 5: Comparison of two-dimensional fits for NP contributions to $\{C_9^\mu, C_{10}^\mu\}$ using all available $b \to s\ell\ell$ data. The darker (lighter) coloured regions correspond to 68% (95%) CL fit results. See the main text for the definition and relevant reference for each group.

- HMMN: T. Hurth, F. Mahmoudi, D. Martínez-Santos, S. Neshatpour [27].

Fig. 5 shows the two-dimensional fit result for all $bs\ell\ell$ observables. While there are differences in experimental inputs, form factors, assumptions on non-local matrix elements and statistical frameworks considered by different groups, the figure shows a good agreement between the fits from most of the groups.

4. Conclusions

The current agreement of the clean observables R_K, R_{K^*}, and BR($B_s \to \mu^+\mu^-$) with the SM implies tight restrictions on new physics contributions in $b \to s\ell^+\ell^-$ decays, enforcing lepton flavour universality, and constraints from BR($B_s \to \mu^+\mu^-$) on the axial Wilson coefficient C_{10}. Our analysis reveals that while a two-dimensional fit $\{C_9^\mu, C_{10}^\mu\}$ (with C_9^e and C_{10}^e kept at their SM values) suggests a preference for new physics in C_9^μ, and to a lesser extent in C_{10}^μ, caution is warranted in interpreting this fit due to its inconsistency with recent $R_{K^{(*)}}$ measurements, indicating a lepton flavour universality violating solution.

However, the tensions observed in angular observables and branching ratios remain untouched by the latest LHCb measurements. These tensions are most plausibly explained by a lepton flavour universal new physics effect in the Wilson coefficient C_9, particularly pronounced in the low-q^2 observables, notably in the $[6-8]$ GeV^2 bin. This region is highly sensitive to C_9 contributions but susceptible to contamination from charm-loop effects.

Furthermore, employing the Wilks' test, we find that new physics contributions in C_9 offer the most viable explanation for the observed tensions in $b \to s$ decays, with no significant improvement

in the fit observed when considering more complex models with additional degrees of freedom.

References

[1] LHCb collaboration, *JHEP* **08** (2017) 055; *Nature Phys.* **18** (2022) 277.

[2] G. Hiller and F. Kruger, *Phys. Rev. D* **69** (2004) 074020.

[3] M. Bordone, G. Isidori and A. Pattori, *Eur. Phys. J. C* **76** (2016) 440.

[4] LHCb collaboration, *Phys. Rev. Lett.* **111** (2013) 191801.

[5] LHCb collaboration, *JHEP* **06** (2014) 133.

[6] LHCb collaboration, *JHEP* **06** (2015) 115.

[7] LHCb collaboration, *JHEP* **09** (2015) 179.

[8] LHCb collaboration, *JHEP* **02** (2016) 104.

[9] LHCb collaboration, *Phys. Rev. Lett.* **125** (2020) 011802.

[10] LHCb collaboration, *Phys. Rev. Lett.* **126** (2021) 161802.

[11] LHCb collaboration, *JHEP* **11** (2021) 043.

[12] LHCb collaboration, *Phys. Rev. Lett.* **127** (2021) 151801.

[13] C. Bobeth, M. Chrzaszcz, D. van Dyk and J. Virto, *Eur. Phys. J. C* **78** (2018) 451.

[14] N. Gubernari, D. van Dyk and J. Virto, *JHEP* **02** (2021) 088.

[15] N. Gubernari, M. Reboud, D. van Dyk and J. Virto, *JHEP* **09** (2022) 133.

[16] Y. Monceaux, A. Carvunis and F. Mahmoudi, *PoS* **FPCP2023** (2023) 060

[17] CMS collaboration, *Phys. Lett. B* **842** (2023) 137955.

[18] ATLAS collaboration, *JHEP* **04** (2019) 098.

[19] LHCb collaboration, *Phys. Rev. D* **105** (2022) 012010.

[20] LHCb collaboration, *Phys. Rev. Lett.* **128** (2022) 041801.

[21] S. Neshatpour, T. Hurth, F. Mahmoudi and D. Martinez Santos, *Springer Proc. Phys.* **292** (2023) 11.

[22] LHCb collaboration, *Phys. Rev. D* **108** (2023) 032002.

[23] T. Hurth, F. Mahmoudi, D.M. Santos and S. Neshatpour, *Phys. Lett. B* **824** (2022) 136838.

[24] F. Mahmoudi, *Comput. Phys. Commun.* **178** (2008) 745; *Comput. Phys. Commun.* **180** (2009) 1579; *Comput. Phys. Commun.* **180** (2009) 1718.

[25] S. Neshatpour and F. Mahmoudi, *PoS* **TOOLS2020** (2021) 036;
PoS **CompTools2021** (2022) 010.

[26] T. Hurth, F. Mahmoudi and S. Neshatpour, *Nucl. Phys. B* **909** (2016) 737.

[27] T. Hurth, F. Mahmoudi and S. Neshatpour, *Phys. Rev. D* **108**, no.11 (2023) 115037.

[28] LHCb collaboration, *Phys. Rev. Lett.* **128** (2022) 191802.

[29] Particle Data Group collaboration, *PTEP* **2022** (2022) 083C01.

[30] J. Bhom, M. Chrzaszcz, F. Mahmoudi, M. T. Prim, P. Scott and M. White, *Eur. Phys. J. C* **81**, no.12 (2021) 1076.

[31] M. Algueró, A. Biswas, B. Capdevila, S. Descotes-Genon, J. Matias and M. Novoa-Brunet, *Eur. Phys. J. C* **83** (2023) 648.

[32] W. Altmannshofer and P. Stangl, *Eur. Phys. J. C* **11**, no.10 (2021) 952.

[33] M. Ciuchini, M. Fedele, E. Franco, A. Paul, L. Silvestrini and M. Valli, *Phys. Rev. D* **107** (2023) 055036.